# Three-step $H^-$ charge exchange injection with a narrow-band laser

V. Danilov, A. Aleksandrov, S. Assadi, S. Henderson, N. Holtkamp, T. Shea, and A. Shishlo
*Spallation Neutron Source Project, Oak Ridge National Laboratory, 701 Scarboro Road, Oak Ridge, Tennessee 37830, USA*

Y. Braiman, Y. Liu, J. Barhen, and T. Zacharia
*Center for Engineering Sciences Advanced Research, Computing and Computational Sciences Directorate, Oak Ridge National Laboratory, Oak Ridge, Tennessee 37830, USA*

(Received 21 May 2002; revised manuscript received 10 March 2003; published 6 May 2003)

This paper presents a scheme for three-step laser-based stripping of an $H^-$ beam for charge exchange injection into a high-intensity proton ring. First, $H^-$ atoms are converted to $H^0$ by Lorentz stripping in a strong magnetic field, then neutral hydrogen atoms are excited from the ground state to upper levels by a laser, and the remaining electron, now more weakly bound, is stripped in a strong magnetic field. The energy spread of the beam particles gives rise to a Doppler broadened absorption linewidth, which makes for an inefficient population of the upper state by a narrow-band laser. We propose to overcome this limitation with a ''frequency sweeping'' arrangement, which populates the upper state with almost 100% efficiency. We present estimates of peak laser power and describe a method to reduce the power by tailoring the dispersion function at the laser-particle beam interaction point. We present a scheme for reducing the average power requirements by using an optical ring resonator. Finally, we discuss an experimental setup to demonstrate this approach in a proof-of-principle experiment.

DOI: 10.1103/PhysRevSTAB.6.053501 PACS numbers: 41.75.Cn

## I. INTRODUCTION

Thin carbon stripping foils are used for $H^-$ charge exchange injection in many existing and planned high-intensity proton synchrotrons and accumulator rings [1]. Stripping foils carry with them undesirable side effects on a high-intensity operation of such rings. Namely, due to multiple traversals of the stripping foil by stored protons, the beam-foil interaction gives rise to uncontrollable beam loss. For the next generation of high-intensity proton rings such as the U.S. Spallation Neutron Source (SNS) [2], the joint JAERI-KEK project (J-PARC) [3], and the European Spallation Source (ESS) [4] among others, this uncontrollable beam loss is a central issue (see, e.g., [5]), since it leads to activation of the accelerator components and complicates routine maintenance of the facility. In addition, there are other undesirable side effects associated with the use of stripping foils, in particular, the reduced reliability due to finite foil lifetime, beam loss and activation associated with partial stripping ($H^-$ to $H^0$) in the foil, and increased ring impedance due to the foil delivery mechanism. Finally, and perhaps most important, it is expected that the lifetime of traditional carbon foils is not sufficient to achieve machine up time goals of future multi-MW proton facilities. For this reason, foil development is an active area of research [1].

Because of these issues, alternative methods of $H^-$ stripping must be explored. Laser-based charge exchange injection methods have been pursued for some time. Laser-stripping injection offers several advantages over traditional carbon foil stripping, principally (i) uncontrollable beam loss from multiple foil traversal is eliminated, (ii) foil lifetime issues are eliminated, and (iii) chopping of the injected beam can be performed by turning the laser beam on and off. In addition, the beam coupling impedance of a laser-stripping injection region is smaller than that, which incorporates a stripping foil and ancillary delivery hardware.

A ''foil-less'' charge exchange injection method was proposed by Zelenskiy *et al.* [6]. In this scheme, the first electron is removed by photodetachment or a field-dissociation process. The hydrogen atom beam is polarized and excited by a laser beam. The remaining electron is removed by photoionization. This scheme requires an impractically large laser power, which is indeed the central difficulty involved in ionizing neutral hydrogen. A more feasible scheme, proposed by Yamane [7], consists first of Lorentz stripping of $H^-$ in a strong magnetic field producing neutral atomic hydrogen, followed by laser excitation from the $n = 1$ to the $n = 3$ state, and finally, Lorentz stripping of the excited hydrogen atoms yielding protons. The difficulty in this scheme arises from the finite momentum spread of the beam. The $n = 1$ to $n = 3$ transition is Doppler broadened to a width which is well beyond that achievable with present-day lasers, so only a small fraction of the beam is excited to the $n = 3$ state by a narrow-band laser setup.

We present in this paper a feasible three-step laser-stripping scheme that overcomes the difficulty of the Doppler broadened absorption linewidth. We enhance this scheme further by making use of a tailored dispersion function at the injection point to reduce the Doppler broadening. We then explore possibilities for reducing the required laser power further with the use of an optical ring resonator. Finally, we discuss the practical

  

realization of such an injection scheme in a high-intensity proton ring and in a proof-of-principle experiment. Throughout the paper we will use the SNS parameters as an example, although this scheme is generally applicable to any high-intensity proton ring.

## II. LORENTZ STRIPPING OF $H^-$ IONS AND $H^0$ EXCITED STATES BY A MAGNETIC FIELD

A transverse magnetic field in the laboratory frame produces an electric field in the rest frame of the $H^-$ ions according to the Lorentz transformation of the fields:

$$|E_\perp| = \beta\gamma c|B_\perp|, \tag{1}$$

where $\beta = v/c$, $\gamma = (1-\beta^2)^{-1/2}$, $v$ and $c$ are the velocities of the $H^-$ ion and light, respectively, and $B$ is the magnetic field. The electric field in the rest frame modifies the potential well for the bound electrons and leads to their possible escape from the region of the potential minimum. For 1 GeV $H^-$ ions a magnetic field of several kilogauss is enough to strip one electron, due to the small binding energy (0.755 eV). On the other hand, a magnetic field of order 40 T is required to strip the remaining electron in the $H^0$ ground state due to the large binding energy (13.6 eV). Therefore, additional measures must be taken to facilitate stripping of the hydrogen atom. It was suggested in [7] that one possible way to strip the last electron is to excite the atomic hydrogen to the $n = 3$ state by resonant laser excitation. The excited states of hydrogen are much easier to strip by a magnetic field. For example, the $H^0$ $n = 3$ state electron is more weakly bound than the extra electron in an $H^-$ ion. This implies that similar magnets can be used for both the $H^-$ ion and the $H^0$ excited state ($n > 3$) stripping.

Without using complicated nonlinear magnetic fields, Lorentz stripping produces an increase in the transverse angular spread of the beam due to the probabilistic nature of the stripping process. To choose the required magnetic field configuration we use a simplified criterion: the magnetic stripping scheme is satisfactory if the angular spread induced by stripping is comparable to the inherent angular spread in the $H^-$ beam delivered from the linear accelerator. We now estimate the required magnetic field using this criterion.

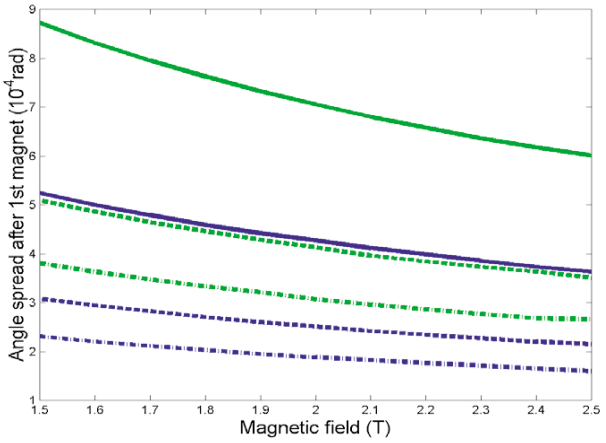


FIG. 1. (Color) Angular spread vs field for 1 GeV (solid lines), 1.3 GeV (dashed lines), and 1.5 GeV (dash-dotted lines) $H^-$ beam energies for the magnet gap 2 cm (blue lines) and 4 cm (green lines).

The average angular deflection $\varphi$ in an arbitrary magnetic field $B(s)$ (assuming small change in the transverse coordinate and assuming exponential conversion of $H^-$ to $H^0$) is given by

$$\varphi = \int_0^\infty \frac{ds}{\beta c\gamma\tau(s)} \exp\left(-\int_0^s \frac{ds'}{\beta c\gamma\tau(s')}\right)\cdot \int_0^s \frac{ds'}{\rho(s')}, \tag{2}$$

where $\tau(s) = [A_1/\beta\gamma c|B(s)|]\exp[A_2/\beta\gamma c|B(s)|]$ is the lifetime of $H^-$ in the rest frame of the ion (see, e.g., [8]), with $A_1 = 2.47 \pm 0.09 \times 10^{-14}$ MVs/cm, $A_2 = 44.94 \pm 0.10$ MV/cm, and $\rho(s) = [\gamma m v/eB(s)]$ is the radius of curvature of the $H^-$ ion trajectory in the magnetic field $B(s)$. The rms spread $\sigma_\varphi$ of the angles is given by

$$\sigma_\varphi = \sqrt{\int_0^\infty \frac{ds}{\beta c\gamma\tau(s)} \exp\left(-\int_0^s \frac{ds'}{\beta c\gamma\tau(s')}\right)\cdot\left(\int_0^s \frac{ds'}{\rho(s')} - \varphi\right)^2}. \tag{3}$$

Figure 1 shows the angular spread introduced by Lorentz stripping of $H^-$ as a function of a central magnetic field in a dipole magnet with gaps of 2 and 4 cm. Curves for three different energies are shown. Taking the SNS injection region as an example with $\beta = 10$ m, the angular spread is $\sigma_\varphi = 0.16$ mrad, which is similar to the presented in the figure numbers.

One important consideration of the stripping scheme is that if the laser light is oriented in the horizontal plane, the stripping should be done in the vertical plane (and vice versa) in order to avoid the influence of the resulting angular spread due to the Doppler effect[1] on the laser frequency in the rest frame of the hydrogen atoms.

As for stripping the remaining electron from the excited states of hydrogen, it was noticed in [7] that the $n =$

[1]Addition of a small vertical angle does not change the total angle between the laser and the hydrogen beams in the first order of this angle.

3 state of $H^0$ has nearly the same dependence of the lifetime on the magnetic field (even more steep dependence), therefore the excited hydrogen atoms can be stripped with a similar 2 T magnet.

## III. LASER EXCITATION OF HYDROGEN FROM THE GROUND TO UPPER STATES

When a hydrogen atom is placed in a laser beam with frequency equal to the transition frequency between the ground and excited state, the electron wave function starts to oscillate between the two states with a frequency (the Rabi frequency) proportional to the amplitude of the laser electric field. We take the formulas for the Rabi frequency from [7] and use them for the states $n = 1$ and $n = 3$. One can find the detailed calculations in [9]. The Rabi frequency is

$$\Omega = \frac{3^3 e a_0}{2^6\sqrt{2}}\sqrt{\frac{2Q_0}{c\varepsilon_0}}/\hbar, \tag{4}$$

where $\varepsilon_0$ is the permittivity of free space, $Q_0$ is the laser power density in $W/m^2$, and $a_0$ is the Bohr radius. The excited state has quantum numbers $n = 3$, $l = 1$, $m = 0$, if the light is polarized in the vertical direction. The Rabi frequency formula for all levels is presented in the next section.

The advantage of excitation through an intermediate excited state is that the interaction cross section is very high for this type of resonant excitation, compared with direct electron photodetachment. The photodetachment process has a broad spectrum and is not assisted by resonant phenomena, so laser power densities orders of magnitude larger are required.

The resonant laser excitation process, however, has its own drawbacks. First, the process requires Rabi frequencies larger than the inverse decay time of the upper state. The lifetime of the $n = 3$ state, for example, is about 5 ns. This means that the device for excitation should be much shorter than the decay length, which is equal to 1.5 m at 1 GeV. For our laser parameters the interaction region will be about 1 cm, therefore this limitation is readily overcome.

A more fundamental problem is the Doppler broadening of the hydrogen absorption linewidth due to the finite momentum spread of the beam. The laser wavelength, $\lambda_0$, in the $H^0$ atom rest frame is related to the wavelength, $\lambda$, in the laboratory frame as follows:

$$\lambda_0 = \frac{\lambda}{\gamma(1 + \beta\cos\alpha)}, \tag{5}$$

where $\alpha$ is the angle between the laser and the $H^0$ beam in the laboratory frame. For the $n = 3$ upper state the required wavelength is $\lambda_0 = 102.6$ nm. Since the neutral hydrogen beam inherits the energy spread of the $H^-$ beam (which is typically a few times $10^{-4}$), each individual atom has its own excitation frequency in its own rest frame. The relative spread of frequencies is about the same as the spread of particle energies, therefore its absolute value is $\sim 10^{12}\text{sec}^{-1}$. The achievable Rabi frequency is about $10^{11}\text{sec}^{-1}$. It is shown in Ref. [10] that the upper state remains virtually unpopulated if the difference between the laser and the transition frequency is larger than the Rabi frequency. But in our case the spread is much larger than the Rabi frequency and a narrow-band laser can excite only a small fraction of the atoms into the upper state. To overcome this difficulty, it is suggested in Ref. [7] to use a broad-bandwidth laser to cover the whole range of the hydrogen transition frequencies. If this is accomplished with a laser having many lines in its spectrum, it can excite more of the beam; however, we require nearly 100% of the atoms to have simultaneously $\pi$ phase advance of Rabi oscillation in order to achieve good stripping efficiency, which is problematic. The solution for this problem was not presented. We will now present a solution that excites all of the atoms in a realistic beam with energy spread to achieve an excitation efficiency of nearly 100%. The solution to this problem consists of two major elements. First, a method to excite all the atoms nearly simultaneously is presented. Second, we present a method to significantly reduce the absorption linewidth due to the beam energy spread by tailoring the dispersion function at the laser-particle beam interaction region.

## IV. ACHIEVING NEARLY 100% EXCITATION EFFICIENCY WITH A NARROW-BAND LASER

Consider the arrangement shown in Fig. 2. Stripping magnets of the type mentioned above are placed on either side of a laser-particle beam interaction point. The first magnet strips the first electron, and then the neutral hydrogen beam is excited by a laser beam. By preparing a *diverging laser beam*, the angle of incidence of the laser light changes along the hydrogen beam path in the

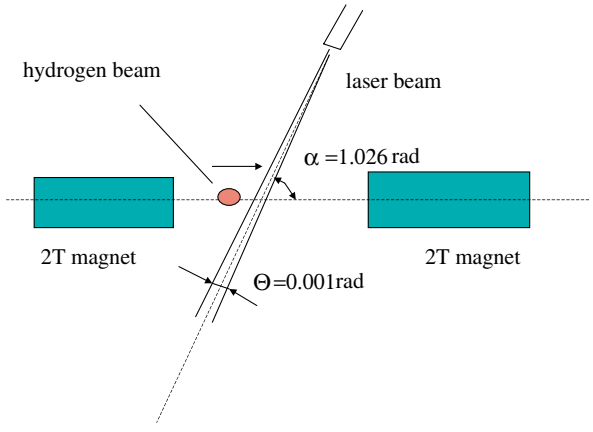


FIG. 2. (Color) Experimental setup for laser excitation of the hydrogen beam (top view). Total length of the region is about 60 cm.

laser-particle beam overlap region. The laser frequency remains fixed, but because of the Doppler dependence of the rest-frame laser frequency on incident angle, the frequency of the light in the atom's rest frame decreases as the angle increases. This introduces an effective frequency "sweep" as the hydrogen beam traverses the laser interaction region, which can be made large enough so that all atoms with differing energies will eventually cross the resonant frequency and will be excited.

To check the degree of excitation we solve the quantum mechanical problem with the laser frequency linearly changing in time. The equation for this is derived in, e.g., [9,10], except for the fact that now the difference of the laser and transition frequencies is a linear function of time:

$$\dot{C}_1 = \frac{i\mu_{1n}E^*}{2\hbar}C_n e^{i\Gamma t^2/2}, \qquad \dot{C}_n = \frac{i\mu_{n1}E}{2\hbar}C_1 e^{-i\Gamma t^2/2}, \quad (6)$$

where $C_1$, $C_n$ are probability amplitudes to be in state 1 or $n$, respectively, $\Gamma = d\omega_0/dt$ is the frequency sweep rate, $\mu_{1n} = \mu^*_{n1} = -\int d^3r u^*_1(\vec{r})ezu_n(\vec{r})$ (assuming the light is polarized and the electric field is parallel with the axis, perpendicular to the plane of Fig. 2), and $u_1$ and $u_n$ are the normalized wave functions of the ground and the upper excited states, respectively. Froissart and Stora [11] obtained the full solution to this problem in connection with electron spin motion. The initial conditions for the problem are $C_1 = 1$, $C_n = 0$. The equations (6) are integrated from $t = -\infty$ to $t = \infty$. The probability $C_n^2$ for the system to finish in the upper state is

$$C_n^2 = 1 - \exp\left(-\frac{\pi\Omega^2}{2\Gamma}\right), \quad (7)$$

where $\Omega = \mu_{1n}\sqrt{(2Q_0/c\varepsilon_0)}/\hbar$ is the Rabi frequency, and $Q_0$ is the laser power density in $\mathrm{W/m^2}$. One can see that if the frequency sweep rate $\Gamma$ is small, the atoms are excited to the upper state, and vice versa. The exponential dependence of the excitation probability on the parameters makes it easy to approach 100% excitation efficiency. We now present the calculation for realistic laser and hydrogen beams. We first present an analytic estimate and then proceed to estimate the required laser power based on a simulation.

As an example, consider the output beam parameters of the 1 GeV SNS linac, summarized in Table I. There are two energy spread values mentioned in the Table. The rms energy spread is the inherent energy spread within a single linac microbunch. In SNS operation, the centroid energy of individual linac bunches will be modulated to accomplish phase-space painting in the energy-phase plane. The magnitude of this momentum painting is also given. We focus on the individual linac bunch energy spread in order to explain the method, since this is representative of many synchrotrons and rings.

We consider a setup in which the Lorentz stripping is accomplished by vertical bending dipoles as described in Sec. II, and the laser beam covers the vertical dimension of the particle beam, i.e., the laser beam lies in the plane of the machine. We assume an interaction time 100 times less than the $n = 3$ state decay time, namely, $T = 0.05$ nsec. Finally, we choose a XeCl excimer laser with wavelength $\lambda = 308$ nm. Given this wavelength, the angle between the hydrogen and the laser beam must be $\alpha = 58.8°$ in order to achieve a 102.6 nm wavelength in the hydrogen atom rest frame.

The first step is to determine the Rabi frequency from Eq. (7). Requiring more than 99% excitation efficiency, the exponent in Eq. (7) should be approximately equal to $-5$, which gives

$$\frac{\pi\Omega^2}{2\Gamma} = \frac{\pi\Omega^2 T}{2\kappa\omega_0} = 5, \quad (8)$$

where $\kappa = 10^{-3}$ is the relative frequency sweep along the beam path, which is taken to be 3 times as large as the relative energy spread of the beam to cover all the particles. This is achieved by making the intersection angle $\theta$ between the laser and hydrogen beam (shown in Fig. 1) change along the hydrogen beam path from $-0.5$ to $+0.5$ mrad. For our parameters this gives a value for the Rabi frequency of $\Omega = 1.08 \times 10^{12}\ \mathrm{sec^{-1}}$ and a laser power density of $Q_0 = 2.703 \times 10^8\ \mathrm{W/cm^2}$ in the rest frame of the hydrogen beam. In the laboratory frame the laser density is smaller by about a factor of 10 and is given by

$$Q = Q_0/\gamma^2(1 + \beta\cos\alpha)^2. \quad (9)$$

The total area of the laser beam is $S = T\gamma c 2\Delta \times \sin(\alpha)\pi/4 \approx 0.84\ \mathrm{cm^2}$, where $\Delta = 1.9$ mm is the vertical size of the laser beam, taken to be slightly larger than the $H^0$ beam with the size of 1.8 mm (see Table I). The

TABLE I. Linac beam parameters at the SNS injection point.

| | |
|---|---|
| Kinetic energy (GeV) | 1.0 |
| $H$, $V$ rms emittance ($\pi$ mm mrad) | 0.26 |
| $\beta_x$, $\beta_y$ (m) | 10.4, 12.1 |
| Horizontal, vertical beam sizes (mm) | 1.6, 1.8 |
| Horizontal, vertical angular divergences (mrad) | 0.16, 0.15 |
| Relative rms energy spread without momentum painting | $0.3 \times 10^{-3}$ |
| Relative energy spread with momentum painting | $\pm 4.0 \times 10^{-3}$ |

horizontal size $\sin\alpha T\gamma c \approx 3.1$ cm is not equal to the vertical size in this particular case. Having presented all the steps of the laser power calculations, it is worthwhile to give a simplified formula for the laser peak power assuming an elliptical laser beam with constant density, a vertical half axis equal to $\Delta$, and a horizontal axis, equal to $\sin\alpha T\gamma c$:

$$P_{\text{peak}} = \frac{\ln(1/\delta)\hbar^2\varepsilon_0 c^2\kappa\omega_0 \sin\alpha\Delta}{2\mu_{1n}^2\gamma(1+\beta\cos\alpha)^2}, \tag{10}$$

where $\delta \ll 1$ is the ratio of unexcited and excited atoms ($\delta \approx 0.0067$ in our case), and $\omega_0$ is the laser frequency in the rest frame of the atom. $\mu_{13} = -\int d^3 r u_1^*(\vec{r}) ez u_3(\vec{r}) = (3^3 e a_0/2^6\sqrt{2})$ for the transition between 1st and 3rd states. One can see that the power does not depend on the horizontal extent of the beam; therefore one can take it to be equal to the vertical size for simplicity. This formula yields the value of about 24 MW for our set of parameters. If one relaxes the stripping efficiency to 95%, the needed power reduces to 14.4 MW. Therefore, before optimizing parameters, we require a peak laser power, which is achievable with commercially available excimer lasers capable of providing 50 MW peak power.

The above calculations were done for constant power density over the laser beam spot. This approximation is not very accurate because the diffraction leads to additional angular divergence of the beam and the real beam with a smoother distribution excites the upper state more adiabatically. For this reason we have performed a more realistic simulation, the results of which are presented in Appendix A. The rms laser beam size is taken to be 1.36 mm. This is the rms transverse dimension of the Gaussian profile for the laser beam intensity. For the electric field, the transverse rms beam extent is $\sqrt{2}$ times larger than the rms laser beam size (the laser light power is proportional to the electric field squared). Therefore, the laser beam electric field rms size is equal to 1.9 mm, which covers the 1.8 mm rms beam size. The rms angular divergence of the laser beam is 0.7 mrad. The other parameters of the Gaussian beam are given in Appendix A. The total required power, integrated over the laser beam cross section, equals 9 MW, though the beam is round in this case and the laser power density is higher than in the previous example of the uniform density beam. With these parameters the estimated excitation efficiency is above 95%.

For comparison, commercially available excimer lasers have 50 MW peak power, but with average power capability of only about 300 W. We discuss in the next section a method to further reduce the power required for efficient excitation.

In addition to the calculated power requirements, the tolerances and alignment requirements of the laser beam should be held at least an order of magnitude less than the divergence angle, i.e., less than the beam angular spread of 0.16 mrad.

## V. REDUCING THE LASER POWER BY TAILORING THE DISPERSION FUNCTION AT THE INTERACTION POINT

Further reduction in the laser power can be achieved by introducing a finite dispersion-function derivative at the laser-particle beam interaction point to eliminate the Doppler broadening of the absorption linewidth. The trajectory of a particle with relative momentum deviation, $dp/p_0$, is displaced by an amount $x = Ddp/p_0$ and has an angle $x' = D'dp/p_0$ with respect to the reference trajectory, where $D$ is the dispersion function, and $D'$ is the derivative of the dispersion function with respect to the longitudinal coordinate. The details on these functions can be found in [13].

The frequency of the laser light in the hydrogen atom rest frame is

$$\nu_0 = \nu\gamma(1+\beta\cos\alpha), \tag{11}$$

where $\alpha$ is the angle between the laser and $H^0$ beam in the laboratory frame and $\nu$ is the laser frequency in the laboratory frame. The angle $\alpha$ between the laser beam and the particle trajectory is $\alpha = \alpha_0 - x'$, where $\alpha_0$ is the angle for the reference energy particle. From $x' = D'(dp/p_0)$ and $d\alpha = -x'$ we have $(d\alpha/d\gamma) = -D'/\beta^2\gamma$. When we equate the derivative of the rest-frame laser frequency with respect to $\gamma$ to zero, we find the requirement

$$D' = -\frac{\beta+\cos\alpha}{\sin\alpha}. \tag{12}$$

If the dispersion derivative satisfies (12), hydrogen atoms with different energies have the same laser light frequency in their rest frames. Figure 3 shows the experimental setup in this case. If compared to the previous setup, shown in Fig. 2, the laser light does not have a divergence since we assume the spread of Rabi frequency is eliminated (we neglect here the contribution from the beam angular spread).

Provided this condition can be met, the dispersion derivative (12) reduces the needed frequency sweep required to excite all the atoms by about a factor of 3. This arises from the fact that the energy spread of the beam is about $3 \times 10^{-4}$, and the angular spread can typically be done 3 or more times smaller. It reduces the peak laser power by the same factor to achieve the same stripping efficiency. But there still exists the angular betatron spread of the particles and we still have to provide some frequency sweep to achieve efficient excitation. Again considering the SNS example, a dispersion derivative $D' = 1.6$ is required for complete cancellation.

Using the SNS parameters as an example, we require peak laser power of 3 MW with the appropriate dispersion

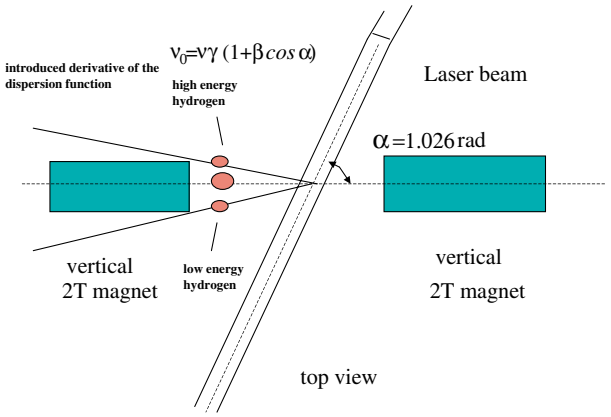


FIG. 3. (Color) Interaction region setup for the elimination of the Doppler broadening. Total length of the region is about 60 cm.

derivative. The average power of the laser will be estimated in the next section.

The required peak laser power is reduced in proportion to the vertical beam size in the case when the laser beam is oriented in the plane of the machine. Lower peak laser powers can therefore be achieved by introducing a small vertical beam waist at the laser-hydrogen interaction point.

Recycling the laser beam as described in the next section can reduce the average laser power further.

## VI. OPTIMAL LASER SETUP TO REDUCE AVERAGE LASER POWER

A high-$Q$ optical ring resonator is proposed as a possible method for reducing the required laser power. Figure 4 shows schematically how such a resonator works. The pulsed light output from the injection-locked XeCl laser is linearly polarized ($p$ polarization) and will be transmitted into the resonator through the polarization beam splitter (PBS). A Pockels cell is appropriately mounted in the resonator to control the polarization state of the light inside the resonator. When the control voltage of the Pockels cell is set to a certain level, $V_\pi$, the polarization axis of the output light will be at 90° to that of the injected light, i.e., the output light will be changed to be $s$ polarized. The control voltage is reset to 0 after a time interval that matches the pulse width. As a result, the injected light is totally changed to the $s$ polarization and will stay in the ring resonator since the PBS completely reflects the $s$-polarized beam. Finally, after a certain time interval, the control voltage of the Pockels cell is set to $V_\pi$ again in order to dump the light from the ring resonator. Figures 4(b) and 4(c) illustrate the timing of the control signal of the Pockels cell and the resulting optical signal inside the resonator, respectively. Since the interaction between the atom and the laser beams during the laser-stripping process causes very little loss to the

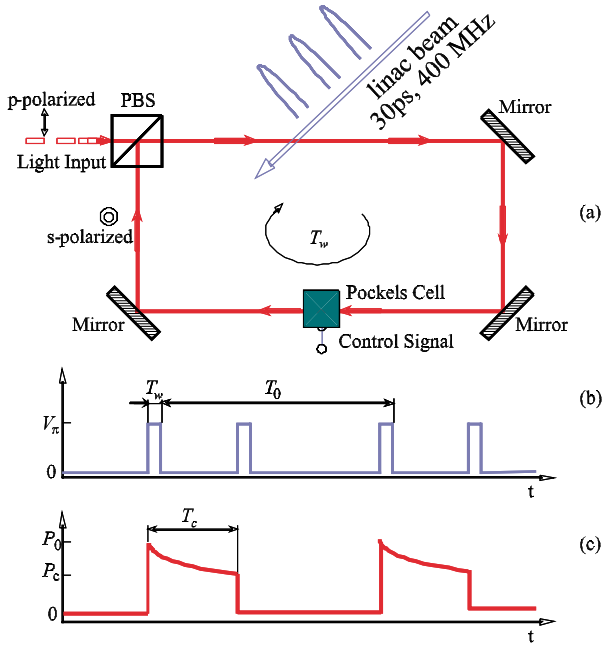


FIG. 4. (Color) Schematic of ring resonator for trapping of optical pulse.

light power, the proposed ring resonator can be used to circulate or to extract the light pulse, as schematically shown in Fig. 4(a). Here, we propose two different implementation methods described as follows.

The first method is to use laser pulses with the repetition rate of 60 Hz that matches SNS's operation cycle. In this implementation scheme, the ring is used to extract the pulse widths of up to 1 ms. Here, the value of $T_0$ in Fig. 4(b) is 1 ms. The resonator length is designed according to the laser pulse width $T_w$ as $L = cT_w/n$, where $n$ is the refractive index of the resonator and $c$ is the speed of light. The cavity decay time $\tau_c$ is given by $\tau_c = T_w/\alpha$, where $\alpha$ is the whole resonator loss due to mirror reflection and absorption in one trip. The pulse length $T_c$ in Fig. 4(c) is determined by the time duration in which the light intensity decreases from $P_0$ to $P_c$, a lower level that is set by the required stripping efficiency. Since the light power inside the ring resonator decreases as a function of $\exp(-t/\tau_c)$, $T_c$ is given by $T_c = -\tau_c \ln(P_c/P_0) = (-T_w/\alpha)\ln(P_c/P_0)$. Taking an example of $T_w = 20$ ns, $P_0 = 20$ MW, and $P_c = 400$ kW, to achieve $T_c = 1$ ms, the resonator loss has to be as low as $10^{-4}$ in a 6-m-ring resonator. A possible solution is to include a medium with external pumping in the resonator so that resonator loss can be compensated by the pumping. The average laser power in the ideal situation is 20 MW (peak power) × 20 ns (pulse width) × 60 Hz (repetition rate) = 24 W.

The second method is to use laser pulses with a pulse width of 50 ps that can overlap the linac beam bunch length (30 ps). The repetition rate can be 1 MHz to match the cycle frequency of the accumulator ring. Here, the

ring resonator is used to circulate the short pulse at the frequency of about 400 MHz. In this method, the pulse lifetime in the resonator needs to be 650 ns, which is the "beam-on" time of the linac beam during each 1 $\mu$s chopping cycle. Accordingly, the value of $T_0$ in Fig. 4(b) is 1 $\mu$s in this case. If we use $T_w = 2.5$ ns, $P_0 = 20$ MW, $P_c = 400$ kW, and $T_c = 650$ ns, the resonator loss is calculated to be about 1.5% in a 75-cm-ring resonator which can be much more easily achieved than the first method. The average laser power in this case is 20 MW (peak power) $\times$ 50 ps (pulse width) $\times$ 1 MHz (repetition rate) = 1000 W without a dispersion derivative and the vertical beam size reduction. With the dispersion derivative it will be reduced to 330 W. If the vertical size is reduced by factor of 5 (which is reasonably achievable), the average power will become equal to 66 W. The challenge in this method, however, is due to the power requirement of the light source. Currently, Ti-sapphire or semiconductor lasers are candidates for generating a short pulse with high repetition rates. Upscaling laser power can be achieved by using synchronized laser arrays [14]. Synchronization of a high power, semiconductor laser array has been demonstrated, for example, by employing the injection locking technique [15].

## VII. PRACTICAL REALIZATION IN A PROOF-OF-PRINCIPLE EXPERIMENT AND IN AN ACCUMULATOR RING

We describe the setup and parameters envisioned for a proof-of-principle experiment, which can be carried out in the linac dump transport line at the SNS facility for the 1 GeV $H^-$ beam. The interaction region must have a small vertical beam size. This is easily achievable by a reduction of the beta function to 2.5 m. The magnetic stripping is performed in the vertical direction in order to have a small horizontal angular spread. Since the laser and the hydrogen beams pass through one another in the horizontal plane with a large angle, the horizontal size of the hydrogen beam can be almost as large as the length of the laser beam, i.e., not less than 1 cm. Therefore the horizontal beta function should be as large as possible to minimize the horizontal angular spread. On the other hand, the vertical spread does not cause broadening of the absorption linewidth (see the end of Sec. II). The first stripping magnet should be a strong magnet with a gap of 4 cm and a central field of 2 T or more. The stripping with 2 T adds an additional vertical angular spread for a 1 GeV beam of about $0.7 \times 10^{-3}$ rad, which is about 2 times larger than the linac vertical angular spread at this point, but this does not affect the stripping process (see the end of Sec. II). The second magnet (after the hydrogen excitation) should have the same parameters. It is also desirable to maintain the average bend angle equal to zero.

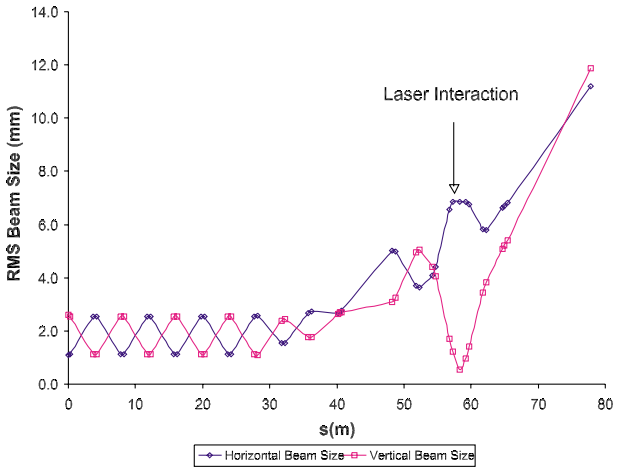


FIG. 5. (Color) Horizontal and vertical rms beam sizes in the linac dump line. The proposed interaction point is indicated.

Figure 5 shows rms beam sizes in the line in which the optical functions have been adjusted to produce a beam waist in the vertical plane and a large horizontal beta function at a location equidistant from nearby quadrupoles. This solution achieves a waist with 1 m of free space on either side of the interaction point. The interaction region rms beam sizes are 0.54 and 6.9 mm for vertical and horizontal, respectively, the horizontal angular spread is about $7 \times 10^{-5}$, and the linac energy spread is about $0.3 \times 10^{-3}$. We do not have the capability to generate significant dispersion in the dump line since it would require additional dipole magnets.

Besides the special magnets and the adjustment of the quadrupoles, electron collectors are needed to detect stripping in the first and the third magnets. Additionally, accurate control of the magnetic field at the interaction point is needed. The laser with the peak power of 50 MW and wavelength around 355 nm is commercially available and not expensive. The details of the proposed proof-of-principle experiment are presented in [9].

A full design implementation of such a laser-stripping system in an accumulator ring is the subject of ongoing work and is beyond the scope of this paper. Indeed, many aspects of the proposed methods require experimental investigation as well as advances in the rapidly evolving field of laser science. Nevertheless, some general implementation issues can be described. First, it is noted that to make use of the dispersion tailoring, it is necessary only that the injected beam dispersion be modified; the accumulator ring dispersion may remain fixed at the expense of some dispersion mismatch. For rings, which utilize phase-space painting, the mismatch is a minor concern. An injection region layout shown in Fig. 6 accommodates the new laser injection scheme. A set of horizontal bending chicane dipoles displaces the stored beam in the ring. The first stripping magnet is placed in the injection line. The neutral hydrogen beam and stored

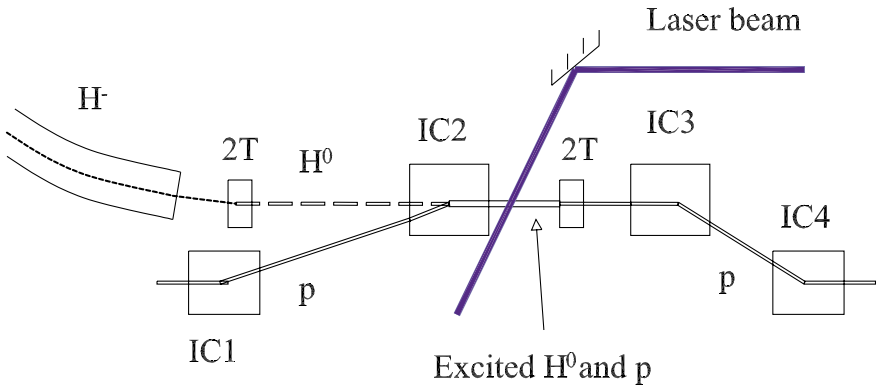


FIG. 6. (Color) Layout of accumulator ring injection region incorporating laser stripping. IC1–IC4 show injection chicane magnets.

proton beam overlap at the laser-particle beam interaction point. The second magnet, an undulator type placed in the ring, strips the remaining electron.

It should be pointed out that for the application in rings that utilize momentum painting (such as the SNS), a large relative energy modulation of about $+/-0.004$ is introduced. Without dispersion tailoring, the peak laser power required is about 720 MW, and the average power with the optimal setup is about 520 W. If dispersion tailoring can be achieved, the required average power is reduced to 14.4 W.

## VIII. CONCLUSION

This paper presents a feasible method for three-step laser-stripping injection. A solution is found which alleviates the difficulty reported in [7], namely, the Doppler broadening of the absorption linewidth due to the particle beam energy spread. By exciting the neutral hydrogen beam in a diverging laser beam, an excitation frequency sweep is introduced which effectively populates the excited state, even for realistic beams with energy spread. Further reduction in the peak laser power requirements was described, based on tailoring the dispersion function at the laser-particle beam interaction point. Some ideas for reducing the average laser power requirements, based on optical ring resonators, were also described.

## ACKNOWLEDGMENTS

This research was sponsored by UT-Batelle, LLC, under Contract No. DE-AC05-00OR22725 for the U.S. Department of Energy. SNS is a partnership of six national laboratories: Argonne, Brookhaven, Jefferson, Lawrence Berkeley, Los Alamos, and Oak Ridge.

## APPENDIX A. UPPER LEVEL EXCITATION FOR A REALISTIC GAUSSIAN BEAM

A realistic laser beam has a Gaussian shape and can be described by the function $U(r)$ [12]:

$$U(\vec{r}) = \frac{W_0}{W(z)}\exp\left(-\frac{r^2}{W^2(z)}\right)\exp\left(-jkz - jk\frac{r^2}{2R(z)} + j\zeta(z)\right), \tag{A1}$$

where $r$ is the transverse coordinate, $z$ is the longitudinal coordinate, $k = \omega/c$, $W(z) = W_0[1 + (z^2/z_0^2)]^{1/2}$, $R(z) = z[1 + (z_0^2/z^2)]$, $\zeta(z) = \tan^{-1}(z/z_0) + \varphi$, $z_0$, $\varphi$ are arbitrary constants, and $W_0 = (\lambda z_0/\pi)^{1/2}$. Here, $z$ stands for the longitudinal distance from the waist, $z_0$ is the beam compression parameter (equivalent to the accelerator beta function at the waist), $W(z)$ is the $\sqrt{2}$ beam size at longitudinal point $z$, and $W_0$ is the size of the laser beam at the waist. From the relation $W_0 = (\lambda z_0/\pi)^{1/2}$, one can see that $\lambda/\pi$ is the analog of the accelerator emittance. The rest of the functions are related to the oscillation phase of the light.

Function (A1) satisfies the Helmholtz equation and it can be used to express the electromagnetic field. If we choose the electric field in the vertical $y$ direction, omitting the time dependence $\exp(j\omega t)$, the expressions for the electric and the magnetic fields are

$$E_x = 0, \qquad E_y = -E_0 U(\vec{r}), \qquad E_z = E_0\frac{x}{z + jz_0}U(\vec{r}),$$
$$H_x = E_0\sqrt{\frac{\varepsilon_0}{\mu_0}}U(\vec{r}), \qquad H_y = 0, \qquad H_z = 0. \tag{A2}$$

To describe the fields in the rest frame of the hydrogen atom, we must transform the fields and coordinates into the new system. Figure 7 shows the coordinate notations. The expressions (A2) for the fields are given in the laboratory frame $xyz$; the new system $x'y'z'$ is shifted in the $z$ coordinate and rotated around the $y$ axis by the angle $\pi/2 - \alpha$. The third system $x''y''z''$ (the hydrogen rest-frame system) is moving along the $x'$ axis with velocity $V$. The resulting transformation from the third to the first system is

$$x = \gamma(x'' + Vt'')\sin\alpha + z''\cos\alpha,$$
$$z = S + z''\sin\alpha - \gamma(x'' + Vt'')\cos\alpha, \qquad y = y'', \tag{A3}$$
$$t = \gamma\left(t'' + \frac{V}{c^2}x''\right),$$

where $S$ is the shift of the interaction point from the laser beam waist, $\alpha$ is the angle determined by the Doppler effect and the $n = 3 - 1$ transition frequency; $\alpha = 58.8°$ for $\lambda = 308$ nm.

Taking into account rotation and Lorentz transformation of the fields, neglecting the longitudinal electric field in (A2) under the assumption that $z \gg x$, neglecting the longitudinal coordinate $z$ change during the interaction, and choosing the coordinates $x''$ and $z''$ equal to zero for the hydrogen atom in its rest frame, we obtain the electric field in the rest frame of the hydrogen atom:

$$E(t'') = E_0\gamma(1 + \beta\cos\alpha)\exp\left(-\frac{y''^2 + (\gamma Vt'')^2}{W_0^2(1 + \frac{S^2}{z_0^2})} + j\omega t''\gamma(1 + \beta\cos\alpha) - jk\frac{y''^2 + (\gamma Vt'')^2}{2S(1 + \frac{z_0^2}{S^2})} + j\varphi\right),$$

where $\varphi$ is the nearly constant phase of the oscillation, $\omega$ is the laser frequency, and $E_0$ is the electric field amplitude at the interaction point in the laboratory frame. $S$ is the distance from the waist to the interaction point. It is assumed to be constant since the calculations show it is much larger than the transverse beam size and its variation along the hydrogen beam path is negligible. The vertical coordinate Gaussian dependence hints that the laser beam vertically should cover the hydrogen beam. For our next calculations, with this in mind, we put $y'' = 0$ for simplicity. Now we take Eq. (6) and substitute the electric field to obtain

$$\dot{C}_1 = \frac{i\mu_{1n}E_0\gamma(1 + \beta\cos\alpha)}{2\hbar}C_n e^{-(t^2/2\sigma_t^2) - i\Delta t},$$
$$\dot{C}_n = \frac{i\mu_{n1}E_0\gamma(1 + \beta\cos\alpha)}{2\hbar}C_1 e^{-(t^2/2\sigma_t^2) - i\Delta t}, \tag{A4}$$

where $\mu_{1n} = -\int d^3r u_1^*(\vec{r})ezu_n(\vec{r}) = (3^3ea_0/2^6\sqrt{2})$ for the $n = 3$ state, $\sigma_t = \{W_0[1 + (S^2/z_0^2)]\}^{1/2}/\sqrt{2}\gamma V\sin\alpha\}$ is the rms time duration of the hydrogen-laser interaction in the rest frame of the hydrogen atom, $\Delta = \omega(d\gamma/\gamma)\{1 + [1 + (1/\gamma^2)]\cos\alpha\} + (\Gamma t/2)$ is the phase dependence on time, and $\Gamma = [k(\gamma V)^2\sin^2\alpha]/\{S[1 + (z_0^2/S^2)]\}$ is the frequency sweep rate. This dependence is of absolute importance—it gives frequency variation of the light in the rest frame of the atom. To determine the stripping efficiency one needs to determine constant $\Gamma$. The laboratory frame electric field distribution rms size is chosen to be 1.9 mm to cover 1.8 mm rms beam size (for dimensions, see Table I). This is equivalent to the rms intensity size $\sigma_\perp = 1.36$ mm. This yields $\sigma_t = (\sigma_e/\gamma V\sin\alpha) = (2\pi/\omega_0)12000$, which equals 12 000 oscillations in the rest frame of the atom.

The next step is to determine $\Gamma$. The instant frequency of the laser beam in the hydrogen rest frame is $\omega_0 + \Gamma t$. To have the frequency sweep of 0.001 (same as in the peak power estimation in Sec. IV) over two $\sigma_t$, one needs to chose $\Gamma = 0.0005(\omega_0/\sigma_t)$. For this set of parameters, the distance from the interaction point to the waist is much larger than the laser beam beta function, i.e., $S \gg z_0$, giving $\Gamma\sigma_t^2 \approx (S/z_0) = 12\pi$. From $W(z) = W_0[1 + (S^2/z_0^2)]^{1/2} = \sqrt{2}\sigma_\perp = 0.0019$ m one obtains the beam size at the waist point as $W_0 = 7.2 \times 10^{-5}$ m. From $W_0 = (\lambda z_0/\pi)^{1/2}$, one can obtain the laser beam beta-function value $z_0 = 0.052$ m. The distance from the waist is $S = 12\pi z_0 \approx 2.0$ m. The angular spread can be estimated as the ratio of the beam size at the interaction point and the distance $S$ to the waist and is approximately equal to 0.7 mrad. Figure 8 shows the excitation probability for particles with different energies as a function of time for the given parameters and for the Rabi frequency of $2.5 \times 10^{12}$ s$^{-1}$[2]. This Rabi frequency corresponds to the maximal laser beam energy density at the center of the laser beam and is chosen in order to have stripping efficiency above 95%. The black line shows the probability of excitation of the particle with reference energy of 1 GeV. The blue line represents the particles with $3 \times 10^{-4}$ frequency deviation from the transition frequency of 1 GeV particle, corresponding to the rms linac energy spread. The green line shows the excitation of particles with the relative frequency deviation of $7.5 \times 10^{-4}$

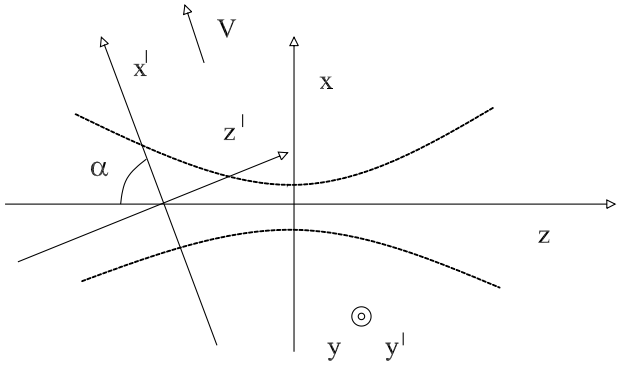


FIG. 7. Coordinate notation for the hydrogen atom in the field of the Gaussian beam.

[2]This number is about 3 times larger than in Sec. IV mostly because the laser beam is round here and it has much larger power density.

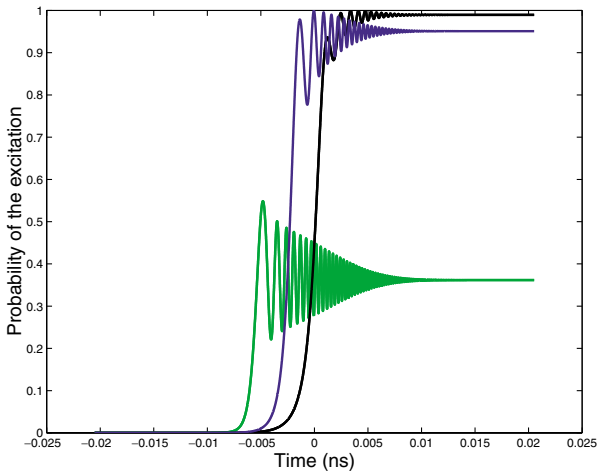


FIG. 8. (Color) Probability of the $n = 3$ excitation versus time for reference energy particle (black line), the particle with the relative energy deviation 0.000 25 (blue line), and 0.000 75 (green line).

(corresponding to 2.5 rms energy deviation) from the reference transition frequency. One can see that even for the particles with one rms energy deviation, the probability of excitation is around 95%, which means that even particles in the tails of the distribution will be efficiently stripped. Obtaining a precise number for the actual stripping efficiency would necessitate the development of a large Monte Carlo simulation code, including the realistic energy and angular distributions. From our simplified simulations, we anticipate the overall efficiency to be better than 95% for the parameters listed above.

As for the laser power, for a round beam with 0.136 cm rms (for the electric field distribution rms is 1.41 times larger), the peak power is 9 MW, similar to what was estimated in Sec. III.

It turns out that if we squeeze the beam horizontally to 50 μm while keeping the laser power the same, the excitation probability also exceeds 90%—in this case without any angular spread. The reason is that the power density becomes so large that the Rabi frequency for all the particles becomes larger than the Doppler spread of the absorption linewidth. In this case all the particles are excited in the same manner. But the required power density needed remains about 10 MW.

[1] I. Yamane, in *Summary Report of Session K on H⁻ Stripping*, Proceedings of the 20th ICFA Advanced Beam Dynamics Workshop on High Intensity and High Brightness Hadron Beams, Batavia, IL, 2002, AIP Conf. Proc. No. 642 (AIP, New York, 2002).

[2] J. Wei *et al.*, in *Proceedings of the 2001 Particle Accelerator Conference, Chicago, 2001* (IEEE, Piscataway, NJ, 2001).

[3] Y. Yamazaki, in *Proceedings of the 2001 Particle Accelerator Conference, Chicago, 2001* (Ref. [2]).

[4] F. H. Bohn, K. Clausen, A. Claver, R. Cywinski, F. Frick, W. Rögener, B. Stahl-Busse, U. Steigenberger, H. Tietze-Jaensch, and P. Tindemans, ESS Project No. ISBN 3-89336-299-1, 2002.

[5] I. Sugai, Y. Takeda, M. Oyaizu, H. Kawakami, Y. Irie, Y. Arakida, I. Yamane, I. Sakai, M. Kinsho, and K. Kuramochi, in *Proceedings of the 20th ICFA Advanced Beam Dynamics Workshop on High Intensity and High Brightness Hadron Beams, Batavia, Illinois, 2002* (Ref. [1]).

[6] A. N. Zelenskiy, S. A. Kokohanovskiy, V. M. Lobashev, N. M. Sobolevskiy, and E. A. Volfert, Nucl. Instrum. Methods Phys. Res., Sect. A **227**, 429–433 (1984).

[7] I. Yamane, Phys. Rev. ST Accel. Beams **1**, 053501 (1998).

[8] *Handbook of Accelerators*, edited by A. Chao and M. Tigner (World Scientific, Singapore, 1998), p. 438.

[9] V. Danilov *et al.*, ORNL Report No. SNS-NOTE-AP-48, 2002.

[10] R. Boyd, *Nonlinear Optics* (Academic Press Inc., New York, 1992), p. 214.

[11] M. Froissart and R. Stora, Nucl. Instrum. Methods **7**, 297–305 (1960).

[12] B. E. A. Saleh and M. C. Teich, *Fundamentals of Photonics* (John Wiley & Sons, New York, 1991), p. 173.

[13] D. A. Edwards and M. J. Syphers, *An Introduction to the Physics of High Energy Accelerators* (John Wiley & Sons, New York, 1993), p. 87.

[14] *Diode Laser Arrays*, edited by D. Botez and D. R. Scifres (Cambridge University Press, Cambridge, England, 1994).

[15] L. Bartelt-Berger, U. Brauch, A. Giesen, H. Huegel, and H. Opower, Appl. Opt. **38**, 5752 (1999); Y. Liu, H. K. Liu, and Y. Braiman, Appl. Phys. Lett. **81**, 978 (2002); Appl. Opt. **41**, 5036 ( 2002).